

1 **DETECTION AND ATTRIBUTION OF FLOOD TRENDS IN MEDITERRANEAN**  
2 **BASINS**

3

4

5

6 Tramblay, Yves<sup>1</sup>

7 Mimeau, Louise<sup>1</sup>

8 Neppel, Luc<sup>1</sup>

9 Vinet, Freddy<sup>2</sup>

10 Sauquet, Eric<sup>3</sup>

11

12 <sup>1</sup> HSM (Univ. Montpellier, CNRS, IRD), 300 Av. du Professeur Emile Jeanbrau, 34090,  
13 Montpellier, France

14 <sup>2</sup> GRED (Univ. Paul Valéry, IRD), 2 rue du Pr Henri Serres, 34000 Montpellier, France

15 <sup>3</sup> IRSTEA, UR RiverLy, Centre de Lyon-Villeurbanne, 5 rue de la Doua CS 20244, 69625  
16 Villeurbanne, France

17

18

19

20

21

22

23 **Version 2, revised manuscript, 20 September 2019**

24

25

26

27

28

29

30

31

32

33 **Abstract**

34

35 Floods have strong impacts in the Mediterranean region and there is a questioning about a  
36 possible increase in their intensity due to climate change. In this study, a large database of 171  
37 basins located in South France with daily discharge data with a median record length of 45 years  
38 is considered to analyze flood trends and their drivers. In addition to discharge data, outputs of  
39 precipitation, temperature, evapotranspiration from the SAFRAN reanalysis and soil moisture  
40 computed with the ISBA land surface model are also analyzed. The evolution of land cover in  
41 these basins is analyzed using the CORINE database. The trends in floods above the 95<sup>th</sup> and 99<sup>th</sup>  
42 percentiles are detected by the Mann-Kendall test and quantile regression techniques. The results  
43 show that despite the increase in extreme precipitation reported by previous studies, there is no  
44 general tendency towards more severe floods. Only for a few basins, the intensity of the most  
45 extreme floods is showing significant upward trends. On the contrary, most trends are towards  
46 fewer annual flood occurrences above both the 95<sup>th</sup> and 99<sup>th</sup> percentiles for the majority of basins.  
47 The decrease in soil moisture seems to be an important driver for these trends, since in most  
48 basins increased temperature and evapotranspiration associated with a precipitation decreases are  
49 leading to a reduction of soil moisture. These results implies that the observed increase in the  
50 vulnerability to these flood events in the last decades is mostly caused by human factors such as  
51 increased urbanization and population growth rather than climatic factors.

52

53

54

55

56

57

58

59

60 **Keywords:**

61 **Floods, trends, France, Mediterranean, soil moisture**

62

63

## 64 **1. INTRODUCTION**

65

66 A number of studies have now established that extreme precipitation could increase due to  
67 climate change in particular in the Mediterranean (Westra et al., 2013, Polade et al., 2017, Ribes  
68 et al., 2018, Trambly and Somot, 2018). Changes in extreme rainfall would be caused by an  
69 increase in the precipitable water content in the atmosphere, related to increasing temperatures,  
70 according to the principle of Clausius-Clapeyron thermodynamics (Drobinki et al., 2016, Pfahl et  
71 al., 2017). Nevertheless, this relationship has a high variability in space, related to temperatures  
72 and available humidity (Wasko et al., 2016). Several studies observed an increase in the number  
73 of dry days associated with increased rainfall intensities, suggesting that dry periods in these  
74 areas would become longer, but that precipitation could be more extreme when they occur  
75 (Paxian et al., 2015, Polade et al., 2017). Nevertheless, the increase in extreme rainfall would not  
76 offset the decrease in precipitation totals, as the drop in cumulative rainfall associated with the  
77 decrease in the frequency of low to moderate rainfall is expected to predominate over the gains  
78 resulting from the intensification of extreme precipitation (Polade et al., 2014).

79

80 Beside changes in precipitation, an increase in rainfall intensity does not necessarily imply an  
81 increase in flood risk (Ivancic and Shaw, 2015, Woldemeskel and Sharma, 2016). Indeed, for a  
82 given rainfall accumulation, the runoff coefficient can be very variable in time and space in  
83 different basins due to complex interactions between precipitation and infiltration processes on  
84 hillslopes which can strongly modulate flood magnitude (Woldemeskel and Sharma, 2016,  
85 Wasko and Sharma, 2017, Bennett et al., 2018). Most global studies on flood trend indicate a  
86 decrease in flood intensity (Do et al. 2017, Wasko and Sharma, 2017, Sharma et al., 2018). Yet,  
87 these trends are highly variable in space for different regions of the globe (Yin et al., 2018, Najibi  
88 and Devineni, 2018). The attribution of these trends is rather uncertain, while Yin et al. (2018)  
89 relate an increase in floods with increased temperatures; Najibi and Devineni (2018) or Hodgkins  
90 et al. (2018) conclude that trends in the flood frequency and duration can be mostly attributed to  
91 long-term climate variability. Nonetheless, as noted by Whitfield (2012), flood generating  
92 processes do not take place at the global but rather a relatively local scale, making generalizations  
93 about flooding in future climates difficult and uncertain. For Mediterranean basins, Blöschl et al.

94 (2017) indicate later winter floods and Mangini et al. (2018) noted a tendency towards increasing  
95 flood magnitude and decreasing flood frequency. These findings are consistent with trends  
96 detected by Mediero et al. (2014) in Spain and Giuntoli et al. (2012) for the South of France.

97  
98 While much work has been done to estimate future climatic conditions, it is not clear about  
99 possible changes in hydrological variables including surface conditions that can strongly  
100 modulate climatic trends (Knighton et al., 2017). In particular, it is known that in many  
101 catchments the initial soil moisture conditions prior to flood events play a key role in flood  
102 generation (Brocca et al., 2008, Trambly et al., 2010, Raynaud et al., 2015, Woldemeskel and  
103 Sharma, 2016, Wasko and Sharma, 2017, Uber et al., 2018, Wasko and Nathan, 2019) and its  
104 temporal change has not been much analyzed up to now. Between two episodes of rain, the base  
105 flow of the perennial rivers originates from the draining of the water contained in the soils and for  
106 some basins from the aquifers. The capacity of the soil to contain water and restore it to generate  
107 runoff depends on its characteristics (e.g. texture, structure, porosity) but also on the amount of  
108 water it already contains at the beginning of a rain episode. Thus, a quasi-saturated soil will not  
109 be able to store a lot of water, which, being unable to infiltrate, will contribute directly to runoff.  
110 In most cases, there is a non-linear relationship between the flow rate and the initial saturation  
111 state of the soil, usually with a threshold value of moisture above which a rapid flow response to  
112 a rainy episode is observed (Norbiato et al., 2008, Viglione et al., 2009, Penna et al., 2011).  
113 Difference in soil types could induce different relationships between floods and initial conditions  
114 (Grillakis et al., 2016, Camarasa-Belmonte, 2016). For intermittent (seasonal runoff only) and  
115 ephemeral streams (runoff only after a rain event), the impact of antecedent soil moisture is more  
116 complex and strongly dependent on the soil type and geological context (in the presence of karst  
117 in particular). In smaller basins, the impact of initial soil moisture content is usually not  
118 significant and it increases with catchment size (Zhang et al., 2011).

119  
120 For some Mediterranean basins, the increase in heavy rainfall associated with a reduced number  
121 of rainy days could decrease the soil water content and therefore increase infiltration capacity,  
122 hence reducing runoff. On the other hand, more intense rains in urbanized, impervious areas or  
123 on bare soils that are subject to crusting effects could increase runoff and therefore the magnitude  
124 of floods. It is therefore necessary to use hydrological or surface models capable of representing

125 these processes. Quintana-Seguí et al. (2011) using the ISBA land surface scheme with different  
126 downscaling methods found a future increase in floods corresponding to a 10-year return level in  
127 southern French basins, but with different magnitudes depending on the basins. Camici et al.  
128 (2017), in a study on the impacts of climate change on floods in central Italy, noted a greater  
129 sensitivity of basins with permeable soils to changing climatic conditions. Similarly, Piras et al.  
130 (2017) in Sardinia found that impermeable and flat sub-basins are predicted to experience more  
131 intense flood events in future scenarios, while more permeable and steep sub-catchments will  
132 have an opposite tendency. However, there are systematic differences between projections of  
133 changes in flood hazard in south Europe (Italy, Greece, Iberian Peninsula) in most European and  
134 global studies using large-scale hydrological models (Kundzewicz et al., 2017). Indeed some  
135 studies points towards an increase in southern Europe (Quintana-Seguí et al., 2011, Alfieri et al.,  
136 2015) while others suggests a decrease (Donnelly et al., 2017, Thober et al., 2018). This is due to  
137 different GCM, RCM, scenarios and downscaling approaches but also the use of large scale  
138 hydrological model usually not calibrated and validated for all basins. This type of global (or  
139 large scale) hydrological model (e.g. LISFLOOD, VIC, HYPE) is usually not adapted to small  
140 river basins less than 500 km<sup>2</sup>, which is the typical catchment size found in the Mediterranean  
141 region.

142  
143 Prior to make future projections on flood hazard, there is a need to understand the main drivers of  
144 changes for floods and the links between floods and climate characteristics (Merz et al., 2014).  
145 Indeed, understanding the potential flood drivers and their changes may be more relevant than  
146 predictions of uncertain flood changes as noted by Blöschl et al. (2015). The objective of this  
147 study is to analyze trends in floods characteristics for a large sample of French Mediterranean  
148 basins and to relate these trends to climate and land use dynamics. This is done using statistical  
149 tests for the detection of trends and quantile regression models to relate high discharge quantiles  
150 to different climatic drivers.

151  
152 **2. DATA**  
153  
154 171 basins located in south France are selected with a minimum of 20 years of daily discharge  
155 data. The selection of basins is based on the availability of long time series of daily discharge and

156 the selected basins have no significant human influence on flow, from a previous database  
157 elaborated from Sauquet and Catalogne (2011) and Snelder et al. (2013). The median record  
158 length is 45 years and 56 stations have more than 50 years of data, more than 100 stations have  
159 complete years, with less than 5% missing data, between 1970 and 2010. All the catchments  
160 selected have a Mediterranean climate, with a precipitation deficit during summer when the low  
161 flows are recorded. These basins are experiencing flash flood events caused by intense rainfall  
162 events, corresponding to the only region in France when rainfall can exceed 200 mm/day  
163 (<http://pluiesextremes.meteo.fr>) with the maximum occurrence between September and  
164 November. Most basins have a catchment area lower than 500 km<sup>2</sup> and located below 1000 m.  
165 (figure 1). The proportion of karstic areas for each basin has been obtained from the BDLISA  
166 database (available here: <https://bdlisa.eaufrance.fr/>) which provides a delineation of karst  
167 systems in France (Schomburgk et al., 2016). Very common geological formation in the French  
168 Mediterranean region, about 50 gauged basins have more than 50% of their catchment areas with  
169 carbonaceous superficial formations, indicative of Karstic areas. This means that the rainfall-  
170 runoff relationship in this type of basin can be strongly modulated by the presence of karst  
171 (Jourde et al., 2007).

172  
173 In addition to daily discharge data, different variables have been retrieved from the SAFRAN-  
174 ISBA-MODCOU (SIM) hydro-meteorological model (Habets et al., 2008). SIM is based on the  
175 SAFRAN reanalysis over France (Quintana-Seguí et al., 2008) based on observed data and  
176 provides rainfall, snowfall, temperature, and reference evapotranspiration for a 8x8km grid over  
177 France at the daily time step from 1958 until present. The SAFRAN reanalysis is used to force  
178 the ISBA land surface scheme of Météo-France (Habets et al., 2008), to provide among other  
179 variables the actual evapotranspiration, the surface and root zone soil moisture at the same spatial  
180 and temporal resolution than ISBA. Trambly et al. (2010) have shown that the soil moisture  
181 from the root zone simulated by ISBA is an appropriate indicator of soil moisture prior to flood  
182 events in French Mediterranean catchments. The catchment boundaries of the 171 basins selected  
183 have been extracted from the HydroSheds database (<https://hydrosheds.org/>) providing flow  
184 accumulation and flow direction maps at the 15 arc-second resolution. Then the total  
185 precipitation, rainfall, air temperature, actual and reference evapotranspiration from SAFRAN

186 and the surface and root zone soil moisture from ISBA have been extracted and averaged over  
187 every catchment.

188  
189 The evolution of landcover between 1990 and 2018 in the 171 basins was analyzed using the  
190 Corine Landcover inventory (CLC1990 and CLC 2018). Corine Landcover provides an inventory  
191 of 44 classes over the European region (Büttner et al., 2002). CLC1990 and CLC2018 are  
192 respectively based on Landsat-5 (50m spatial resolution) and Sentinel-2 (10m spatial resolution)  
193 satellite images. A limitation of the CLC inventory lies in the difference of accuracy between the  
194 CLC1990 and CLC2018 products, which may introduce an uncertainty in the estimation of the  
195 evolution of the land cover in the studied basins.

### 196 197 **3. METHODS**

198  
199 Two approaches are considered to evaluate trends. The first approach, presented in section 3.1  
200 thereafter, relies on the Mann-Kendall test (Mann 1945) applied to the annual number of flood  
201 events above two different percentiles, the 95<sup>th</sup> and the 99<sup>th</sup> computed on the whole time series  
202 and also on the magnitude of these events. Using two different thresholds, which are commonly  
203 used for the analysis of floods, allows considering separately the trends on moderate (above the  
204 95<sup>th</sup> percentile) and more severe (above the 99<sup>th</sup> percentile) flood events.

205  
206 The second approach presented in section 3.2, is based on quantile regression (Koenker and  
207 Basset, 1978) to estimate the temporal trend magnitude in the 95<sup>th</sup> and 99<sup>th</sup> percentiles of daily  
208 runoff in all stations. The quantile regression method is also used to relate the change in runoff  
209 quantiles to changes in climate characteristics, hence providing a way to attribute the observed  
210 changes to their potential drivers.

211  
212 Hydrological years are considered, starting September 1<sup>st</sup> and ending August, 31 of the next  
213 calendar year. Years with more than 5% missing days are removed. For the first approach based  
214 on event characteristics, a de-clustering is required to not include in the flood sample consecutive  
215 daily threshold exceedances that belong to the same flood event. A minimum of 2 days between  
216 two flood events is selected since it is the average duration of rainstorm in the region (Tramblay

217 et al. 2013). This means, if for two consecutive days the runoff is exceeding the threshold, only  
218 the maximum value is retained. Moreover, different values between 1 and 5 days to separate the  
219 events have been tested and did not change the trend results.

220

### 221 **3.1 Test for trends and regional significance**

222

223 The Mann–Kendall (MK) test (Mann 1945) is used for the trend detection. Several studies have  
224 noted that the presence of serial correlation may affect the results of trend analysis by increasing  
225 the variance of the test statistic (Khaliq et al., 2009, Renard et al., 2008). To overcome this  
226 limitation, Hamed and Rao (1998) proposed a corrected MK test statistic considering an effective  
227 sample size that reflects the effect of serial correlation. This correction was applied in the present  
228 study. In addition to the MK test, the method of Sen (1968) is considered to estimate the  
229 magnitude of trends. In the present study, trends are considered significant at the 10% level;  
230 however, sensitivity tests performed for  $p \leq 0.05$ ,  $p \leq 0.01$  revealed very similar spatial trend  
231 patterns.

232

233 The significance level  $\alpha_{local}$  for a statistical test is related to a single test and is no longer valid  
234 when multiple tests are conducted (Wilks 2016). When the number of tests being conducted  
235 increases, more significant values will be found. The goal of the false discovery rate (FDR)  
236 procedure introduced by Benjamini and Hochberg (1995) is to identify a set of at-site significant  
237 tests by controlling the expected proportion of falsely rejected null hypotheses that are actually  
238 true. Renard et al. (2008), Khaliq et al. (2009) or Wilks (2016) demonstrated that the original  
239 FDR is robust to cross correlations between locations and can work with any statistical test for  
240 which one can generate a p-value. This FDR method is applied to the MK test results to check if  
241 the trends are regionally significant. The detected trends are regionally significant if at least one  
242 local null hypothesis is rejected according to the global (or regional) significance level,  $\alpha_{global}$   
243 (Wilks, 2016). For consistency with the local trend analysis, the global significance level is also  
244 set to 10% in the FDR procedure.

245

### 246 **3.2 Quantile regression**

247



248 As a complementary approach to detect trends in quantiles but also to investigate the relationship  
249 between floods and explanatory covariates, the quantile regression (Koenker and Basset, 1978)  
250 method is applied. Quantile regression could be seen as the extension of the ordinary least square  
251 (OLS) regression (Koenker and Machado, 1999, Villarini and Slater 2017). In OLS, the  
252 conditional mean of the response variable is modeled with respect to one or more predictors and  
253 the sum of squared errors is minimized. For quantile regression, a conditional quantile of the  
254 response variable is modelled as function of predictor(s), an asymmetrically weighted sum of  
255 absolute errors is minimized to estimate the slope and intercept terms. In the present work, only  
256 linear relationships are considered with one single covariate at a time, while more complex forms  
257 of dependences could also be considered in quantile regression. The approach has been  
258 previously used to detect trends in extreme precipitation or floods by Villarini and Slater (2017),  
259 Yin et al. (2018) or Wasko and Nathan (2019).

260  
261 Koenker and Machado (1999) introduced the  $R^l$  goodness of fit measure for quantile regression  
262 models. As for the  $R^2$  in the case of OLS,  $R^l$  lies between 0 and 1. Unlike  $R^2$ , which measures the  
263 relative success of two models for the conditional mean function in terms of residual variance,  $R^l$   
264 measures the relative success of the corresponding quantile regression models for a specific  
265 quantile, by comparison with a restricted model (with slope = 0), in terms of a weighted sum of  
266 absolute residuals (see Koenker and Machado, 1999). Consequently,  $R^l$  constitutes only a local  
267 measure of goodness-of-fit for a particular quantile rather than a global measure over the entire  
268 conditional distribution, like  $R^2$ . This measure can help to discriminate between different models  
269 using different covariates (ex: precipitation or temperature). Higher  $R^l$  values indicate that the  
270 model fits better to observations. In this study, this criterion is used to identify the best covariates  
271 that could explain the temporal variations in high runoff quantiles.

272

## 273 **4. RESULTS**

274

### 275 **4.1 Climatic and land cover trends**

276

277 The climate trends have been analyzed on the whole period of available SAFRAN records,  
278 between 1958 and 2018. For each basin, the annual trends in precipitation, rainfall, temperature,

279 soil moisture, actual and reference evapotranspiration have been analyzed with the Mann Kendall  
280 test. From figure 2, It can be seen a significant decrease of annual rainfall in 56 basins, on  
281 average of -20%, accompanied by an increase of the frequency in dry days (with precipitation  
282 below 1 mm) for 46 basins. The snowfall is also decreasing in the same proportions (no shown).  
283 The sole exception where an increase in rainfall is found is for the Asse River at Beyne-  
284 Chabrières on the western foothills of the Alps. This station has long time series spanning from  
285 1983 to 2009, where a +15% trend in annual rainfall is detected over the whole record. Yet, the  
286 detection of this trend might be an artefact since there are several consecutive wet years between  
287 1992 and 2000. This trend in rainfall can be also seen for the soil moisture trends. Associated  
288 with the precipitation decrease, positive temperature trends are observed for almost all basins,  
289 with an average increase of +0.5°C during the time period 1958-2015. Consequently, widespread  
290 increasing trends in reference and actual evapotranspiration rates over all basins are observed,  
291 similarly as in Vicente-Serrano et al. (2014) in Spain or Rivoire et al. (2019) for the whole  
292 Mediterranean region. The combined decrease in precipitation with increased evapotranspiration  
293 yields to a decrease in soil moisture for the surface and the root zone layers. Yet, it must be  
294 stressed here that the soil moisture in the present study is not observed but simulated from the  
295 ISBA land surface model. However, the detected trends are in accordance with previous studies  
296 over South France such as Vidal et al. (2012) or Dayon et al. (2018).

297  
298 About land cover (figure 3), most basins have low urban areas (below 10%) and the basins with  
299 the highest coverage are found mostly in the South East. An increase of urban areas up to +20%  
300 of total catchment surface can be seen between 1990 and 2018 for basins mostly located close to  
301 the Mediterranean coast and in particular in the Provence-Alpes-Côte-d’Azur region. The class  
302 representing discontinuous urban fabric represents 73% of artificialized areas and increased by  
303 +36% between 1990 and 2018. The increase of urbanized areas could have a strong impact on  
304 runoff generation, in particular for small basins, with the increase of impervious surfaces favoring  
305 surface runoff. In contrast, the agricultural and forest land cover can reach 100% of the basin  
306 surface, in particular in the western Tarn regions for agriculture. We can notice a reduction of  
307 forest cover in the Northern Cévennes areas associated with an increase in agricultural surfaces.  
308 When looking in details from the original classification, for some catchments of size 500 km<sup>2</sup> or  
309 less, the percentage of vineyards could exceed 70% of the total catchment areas in particular for

310 basins located in the Occitanie region. For almost all basins, the percentage of vineyards has  
311 decreased between 1990 and 2018. The other dominant land use classes related to agriculture are  
312 pastures (27.8% of all catchments), complex cultivation patterns (21.9%) and land principally  
313 occupied by agriculture with significant areas of natural vegetation (27.7%). Forested areas are  
314 mostly represented by broad-leaved forest (35%), coniferous forest (19%) and mixed forest  
315 (14.4%) classes. It must be noted that the land cover change analysis is hampered by the short  
316 duration of the land use maps available, 28 years between 1990 and 2018, and possibly different  
317 sensors during this period leading the different attribution to some land use classes.

318

## 319 **4.2 Flood trends**

320

321 To analyze flood trends, all flood events above the 95<sup>th</sup> or 99<sup>th</sup> percentiles of daily runoff  
322 computed on the whole time series are extracted. As noted in the method section, a declustering  
323 approach has been implemented to avoid introducing in the samples an autocorrelation signal due  
324 to several consecutive threshold exceedances belonging to the same event. The trend MK test is  
325 applied to the number of annual exceedances above these two thresholds and also on the  
326 magnitude of the threshold exceedances. From figure 4 it can be seen a general tendency towards  
327 a decrease in the annual number of flood events above the 95<sup>th</sup> percentile, that is significant in 67  
328 catchments, and to a lesser extend also in the number of events above the 99<sup>th</sup> percentile in 45  
329 catchments. These trends are regionally significant according to the FDR procedure and  
330 particularly over the northern ridge of the Cévennes mountainous areas. According to the Sen  
331 Slope method to estimate the decrease in the annual number of events above the 95<sup>th</sup> percentile;  
332 for most basins the trends are ranging between -0.5 and -1 event per decade. For the most  
333 extreme cases the trends can reach up to -2.5 events per decade. Since for all catchments the  
334 number of events above the 95<sup>th</sup> percentile per year is 4.5 on average (min =2, max =6, after de-  
335 clustering), the magnitude of these trends can be considered moderate. For the 99<sup>th</sup> percentile the  
336 magnitude of trends are similar, with a maximum decrease of -1.4 events per decade, and for  
337 most stations on average -0.4 events per decade (with an average annual number of 1.6 events  
338 above the 99<sup>th</sup> percentile, after de-clustering). In addition to the trends in the annual number of  
339 events, there is also a weak signal of an increase of the magnitude of floods, in particular above  
340 the 99<sup>th</sup> percentile for 16 stations, yet these trends are not regionally significant.

341  
342 Beside this event-based analysis, the temporal trends in the 95<sup>th</sup> and 99<sup>th</sup> percentiles of the daily  
343 runoff time series have been investigated using quantile regression. The approach is  
344 complementary but different to the testing of trends on the annual occurrence and the magnitude  
345 of the events, since quantile regression allows evaluating the possible changes on the quantiles of  
346 daily runoff time series. This analysis reveals that for a majority of catchments, a decreasing  
347 trend in these two percentiles is detected. The procedure is to apply a quantile regression of the  
348 percentile of interest with time as a covariate, and to validate if the slope of the quantile  
349 regression model is significantly different than zero at the 10% level a bootstrap resampling  
350 approach (Efron, 1979) has been considered. For the 95<sup>th</sup> percentile, a decreasing trend in 147  
351 stations is found and an increase in only 12 stations. For the 99<sup>th</sup> percentile, 89 negative trends  
352 are found and 15 stations with increasing trends. The relative changes in the 95<sup>th</sup> and 99<sup>th</sup>  
353 percentiles are ranging for most stations between 0 and -0.5 as shown on figure 5. The number of  
354 detected trends with quantile regression for the 95<sup>th</sup> and 99<sup>th</sup> percentiles is larger than the number  
355 of trends detected with the MK test. However, for many basins the trends in the 95<sup>th</sup> and 99<sup>th</sup>  
356 percentiles are of small magnitude and only for the largest trends the MK test also detect  
357 significant changes in the annual number of events above these thresholds.

358  
359 In an attempt to relate the detected trends to catchment characteristics, the Student t-test has been  
360 used to compare the catchment descriptors between the group of basins with or without trends.  
361 The catchments where decreasing trends in flood occurrence are detected tend to be are larger  
362 catchments (mean size of 369 km<sup>2</sup> vs. 253 km<sup>2</sup> for the catchments with no significant trends),  
363 with a lower proportion of karstic areas (33% vs. 41%) and urban areas (1.7% vs 3.79%). Also  
364 more decreasing trends are detected in agricultural catchments than in forested areas. Yet, no  
365 clear link can be found between land cover changes and flood trends, probably due to the short  
366 duration of the land cover dataset available. The only exception is about trends in urbanization,  
367 with a lower increase in urbanization (+0.77% average increase in urban areas) in catchments  
368 where floods are decreasing by comparison with catchments with no flood trends (+1.41%  
369 average increase in urban areas). It must be noted that there is a strong spatial variability of the  
370 observed trends highlighting the complex interplays between the different catchment  
371 characteristics, as similarly noted by Snelder et al. (2013) over France. For example, the

372 magnitude of the detected trends is not correlated with the different catchment properties. This  
373 implies that it would be very challenging to propose a typology of basins with similar changes in  
374 floods according to catchment properties.

375

### 376 **4.3 Changes in event precipitation and antecedent soil moisture conditions**

377

378 For each event, the cumulative catchment precipitation average is computed as the sum of non-  
379 zero consecutive rainy days, on a time window up to 10 days prior to the flood event. The  
380 antecedent soil moisture is taken as the root zone soil moisture corresponding to the day prior the  
381 start of the rainfall event. Figure 6 show the Mann-Kendall test results for these two indicators for  
382 floods above the 95<sup>th</sup> and the 99<sup>th</sup> percentiles. An increase of precipitation associated with floods  
383 using both thresholds is observed (for 34 catchments for the 95<sup>th</sup> percentile and 36 catchments for  
384 the 99<sup>th</sup> percentile), associated with a decrease in antecedent soil moisture conditions prior to  
385 floods in up to 40 catchments for floods above the 95<sup>th</sup> percentile. There is a correlation between  
386 the reduction of antecedent soil moisture prior to flood events and the decrease of the annual  
387 number of flood events above the 95<sup>th</sup> percentile ( $r=0.44$ ), also to a lesser extent for the number  
388 of floods above the 99<sup>th</sup> percentile ( $r=0.34$ ). Consequently, as observed in Australia by Wasko  
389 and Nathan (2019) it can be hypothesized that the decrease of antecedent soil moisture is an  
390 important driver leading to the reduction of the annual number of floods, despite the increase in  
391 event precipitation already pointed out by several studies in this region (Tramblay et al., 2013,  
392 Ribes et al., 2018, Blanchet et al., 2018). Indeed, for 12 catchments an increase of event rainfall  
393 is detected when for the same catchments a decrease in the annual number of events above the  
394 95<sup>th</sup> percentile is also observed. It is also the case of 11 catchments for the events above the 99<sup>th</sup>  
395 percentile with an increase of event rainfall accompanied by a decrease in the annual number of  
396 events. However as shown before, the increased event precipitation for several basins is probably  
397 the cause of higher flood magnitudes for the most severe events (above the 99<sup>th</sup> percentile).

398

### 399 **4.4 Explanatory covariates for high runoff quantiles**

400

401 To test the influence of different covariates on the variation of the 95<sup>th</sup> and 99<sup>th</sup> percentile values,  
402 quantile regression models using time, temperature, soil moisture from the root zone, actual

403 evapotranspiration (AE), reference evapotranspiration (ET0) and precipitation have been  
404 compared. The goal here is not to select the best covariates for each station but to identify  
405 relevant covariates at the regional scale. Since climatic covariates could influence the  
406 hydrological response at different time scales (Mediero et al., 2014, Villarini and Slater 2018,  
407 Wasko and Nathan, 2019), three different aggregation periods to compute moving averages have  
408 been compared. For the event scale, the different covariates have been averaged with a 3-day  
409 time lag preceding each event. At the monthly time scale representing the seasonal variability, the  
410 covariates have been averaged for the 30 days preceding the events. For the annual time scale the  
411 covariates have been averaged for 365 days preceding the events. At the event scale, the  
412 precipitation represents the intensity of rainfall during the event than the preceding soil moisture.  
413 On the other timescales, for the monthly and annual aggregation periods the precipitation is here  
414 a proxy for soil moisture and its long term variability. To test which covariate provides the best  
415 reproduction of the observed 95<sup>th</sup> and 99<sup>th</sup> percentiles of the daily discharge time series, the  $R^l$   
416 metric is computed, for each covariate, between the quantile regression model built with the  
417 covariate and a constrained model with a constant slope (0).

418  
419 The results are plotted on figure 9. A similar pattern can be seen for both percentiles, with  
420 decreasing  $R^l$  values for longer time aggregation periods for the covariates. For the event-scale,  
421 both precipitations and soil moisture are outperforming other covariates, including time. The  
422 same results are found for the annual time scale, yet with a different interpretation because annual  
423 precipitation is representing the average level of soil moisture storage rather than event rainfall.  
424 The link observed between the 95<sup>th</sup> and 99<sup>th</sup> percentiles with annual precipitation or soil moisture  
425 is an indication that the long-term decrease observed for these two variables (figure 2) could be  
426 the cause of the observed decrease in the frequency of floods above these two percentiles. At the  
427 monthly time scale, the cumulative precipitation plays the most important role when the effects of  
428 soil moisture, actual evapotranspiration and temperature are similar. For almost all covariates,  
429 there is an improvement by comparison to the quantile regression model using time only.

430  
431 Overall, the  $R^l$  coefficients are decreasing with increasing slopes and basin mean elevation.  
432 However, these two variables are correlated ( $r=0.61$ ). This is an indication that antecedent soil  
433 moisture condition may have a lower influence on flood generation in mountainous areas,

434 probably due to shallower soils and steeper slopes. For event based soil moisture and  
435 precipitation, there is an inverse relationship with basin size: for small basins (less than 500km<sup>2</sup>)  
436 event soil moisture and precipitation are good predictors for the time variations of the 95<sup>th</sup> and the  
437 99<sup>th</sup> percentiles, with  $R^l$  values up to 0.6, when for larger basins the  $R^l$  values are much lower,  
438 reaching a maximum of 0.2 for some basins. When averaged at the monthly or annual time step,  
439 the relation is opposite with a larger influence of soil moisture and antecedent precipitation for  
440 larger basins with higher  $R^l$  coefficients. This finding is fully consistent with results obtained for  
441 different regions of the globe (Zhang et al., 2011, Ivancic and Shaw, 2015, Woldemeskel and  
442 Sharma, 2016, Wasko and Sharma, 2017), highlighting the buffering effects of large basins with  
443 the capacity to store more water than smaller basins.

444

## 445 5. CONCLUSIONS

446

447 The results obtained in the present study show that despite the increase in extreme precipitation  
448 events reported by previous studies over the same domain (Ribes et al., 2018) there is not a  
449 general increase in flood occurrence. Only for a few basins, the intensity of the most extreme  
450 floods is showing significant upward trends. On the contrary, a global tendency towards fewer  
451 annual flood occurrences is observed for events of moderate intensity, above the 95<sup>th</sup> percentile.  
452 The same signal, with a lower magnitude, is also seen for higher floods above the 99<sup>th</sup> percentile.  
453 Overall, there are much more trends detected for the annual occurrence of floods than for their  
454 intensity. It should be also emphasized that the magnitude of these trends remains moderated,  
455 with only a few events less by decade and consequently these trends are only noticeable over  
456 long time periods. The decrease in soil moisture seems to be an important driver for these  
457 detected changes, indeed in all basins an increase of temperature and evapotranspiration  
458 associated with a decrease in precipitation is leading to a reduction of soil moisture over time. For  
459 several basins, the soil moisture decrease can offset the increase in extreme precipitation and  
460 generate less frequent floods. These changes are mostly observed for larger agricultural basins,  
461 with low urbanization and karstic areas. Wasko and Sharma et al. (2017) previously noted the  
462 importance of catchment size for the influence of soil moisture on flood runoff due to higher  
463 potential of soil moisture storage. The trends detected in the present work are consistent with  
464 those found in other Mediterranean regions such as Spain (Mediero et al., 2014) and Australia

465 (Wasko and Nathan, 2019). An important finding of the present work is that with the same large  
466 scale climatic drivers (in terms of temperature, evapotranspiration and precipitation) the flood  
467 trends in the basins can be different. This shows the importance of basins characteristics to buffer  
468 climatic variability. Indeed, even if similar patterns of changes in the 95<sup>th</sup> and 99<sup>th</sup> percentiles are  
469 found, the analysis of individual catchments is revealing spatial differences even for neighboring  
470 basins caused by different topography, soil and land cover combinations. This is a factual  
471 demonstration of the commentary of Whitfield (2012) stating that it would be very difficult, if  
472 not scientifically irrelevant, to make general statements about the plausible future evolution of  
473 flood risk.

474  
475 These results showing a lack of a generalized upward trend in floods should be put into  
476 perspective with the observed increase in the vulnerability to these episodes. Indeed many reports  
477 such as Llasat et al (2013) indicate an increase in the number of floods inducing damages  
478 between 1981 and 2010 in South France and North Spain, which they attribute to an increased  
479 vulnerability and land use changes. The French Mediterranean regions are concentrating 66% of  
480 the total cost of flood damage to private properties in France (Vinet, 2011) and the total assets  
481 lost due to floods are rising as in many other regions (CCR, 2018, Paprotny et al., 2018). The  
482 areas close to the Mediterranean have seen a population increase and an extension of urbanized  
483 areas, driven in part but not solely by the increase of touristic activities (Vinet, 2011, Vinet and  
484 De Richemond, 2017). Bouwer (2011) concluded after a review of 22 disaster loss studies that  
485 there is no trends in flood losses, corrected for changes (increases) in population and capital at  
486 risk, which could be attributed to anthropogenic climate change". Therefore, it can be concluded  
487 that, at least for Southern France, as noted previously by Neppel et al. (2003) the increasing cost  
488 of damages caused by floods is rather due to the increase in socio-economic vulnerability rather  
489 than a climate change signal towards an increase in the severity of floods. Nonetheless, the  
490 evolution of flood frequency and intensity is a key question for risk prevention. Flood related  
491 mortality in the Mediterranean basin is conditioned both by hazards drivers (e.g. rainfall  
492 intensity, discharge) but also by social drivers (behaviors, characteristics of buildings...) as  
493 shown in different studies (Ruin et al., 2008, Vinet, 2011, Boudou et al., 2016). Deeper  
494 knowledge in rainfall and flood trends must be crossed with exposure (e.g. population in flood  
495 prone zones) and vulnerability data (e. g. eldering of population in the future) to anticipate



496 evolution in human mortality in relation with flash floods in the Mediterranean basin (Petrucci et  
497 al. 2017). As pointed out in previous research projects (Merz et al., 2014, Meyer et al., 2014)  
498 there is a need to integrate climate change scenarios with socio-economic change scenarios to  
499 better quantify changes in flood risk. To achieve this task, it is necessary to develop databases on  
500 vulnerability and exposure to be analyzed in conjunction with hydrometeorological data (Saint-  
501 Martin et al., 2018).

502

### 503 **Acknowledgements**

504

505 This work is a contribution to the HYdrological cycle in The Mediterranean EXperiment  
506 (HyMeX) program, through INSU-MISTRALS support. The dataset compiled in this work  
507 are made available to the research community upon request.

508

### 509 **References**

510

511 Alfieri, L., Burek, P., Feyen, L., and Forzieri, G.: Global warming increases the frequency of river floods  
512 in Europe, *Hydrol. Earth Syst. Sci.*, 19, 2247-2260, <https://doi.org/10.5194/hess-19-2247-2015>, 2015.

513

514 Benjamini, Y. and Hochberg, Y.: Controlling the false discovery rate: A practical and powerful  
515 approach to multiple testing, *J. Roy. Stat. Soc. B*, 57, 289–300, 1995.

516

517 Bennett B., Leonard, M., Deng Y., and Westra, S.: An empirical investigation into the effect of antecedent  
518 precipitation on flood volume, *J. Hydrol.*, 567, 435-445, 2018.

519

520 Blanchet, J., Molinié, G., and Touati, J.: Spatial analysis of trend in extreme daily rainfall in southern  
521 France, *Clim Dyn.*, 51, 799-812, 2018.

522

523 Blöschl, G., Gaál, L., Hall, J., Kiss, A., Komma, J., Nester, T., et al.: Increasing river floods: fiction or  
524 reality? *WIREs Water*, 2, 329–344, 2015.

525

526 Blöschl, G., Hall, J., Parajka, J., Perdigão, R.A., Merz, B., Arheimer, B., et al.: Changing climate shifts  
527 timing of European floods, *Science*, 357, 588–590, 2017.

528

529 Boudou, M., Lang, M., Vinet, F., and Cœur, D.: Comparative hazard analysis of processes leading to  
530 remarkable flash floods (France, 1930–1999), *J. Hydrol.*, 541, 533–552, 2016.  
531

532 Bouwer, L. M.: Have disaster losses increased due to anthropogenic climate change? *Bull. Am. Met. Soc.*  
533 92 (1), 39-46, 2011.  
534

535 Brocca, L., Melone, F., and Moramarco, T.: On the estimation of antecedent wetness conditions in  
536 rainfall–runoff modelling, *Hydrol. Processes*, 22, 629–642, 2008.  
537

538 Büttner, G., Feranec, F., and Jaffrain, G.: Corine land cover up-date 2000. Technical report,  
539 Copenhagen: European Environment Agency, 2002.  
540

541 Camarasa-Belmonte, A.M.: Flash floods in Mediterranean ephemeral streams in Valencia Region, *J.*  
542 *Hydrol.*, 541, 99–115, 2016.  
543

544 Camici, S., Brocca, L., and Moramarco, T.: Accuracy versus variability of climate projections for flood  
545 assessment in central Italy, *Climatic Change* 141(2), 273-286, 2017.  
546

547 CCR 2018. Conséquences du changement climatique sur les coûts des catastrophes naturelles en France à  
548 Horizon 2050.  
549 [https://www.ccr.fr/documents/23509/29230/Etude+Climatique+2018+version+complete.pdf/6a7b6120-](https://www.ccr.fr/documents/23509/29230/Etude+Climatique+2018+version+complete.pdf/6a7b6120-7050-ff2e-4aa9-89e80c1e30f2)  
550 [7050-ff2e-4aa9-89e80c1e30f2](https://www.ccr.fr/documents/23509/29230/Etude+Climatique+2018+version+complete.pdf/6a7b6120-7050-ff2e-4aa9-89e80c1e30f2)  
551

552 Dayon, G., Boé, J., Martin, E., and Gailhard, J.: Impacts of climate change on the hydrological cycle over  
553 France and associated uncertainties, *Comptes Rendus Geosciences*, 350(4), 141-153, 2018.  
554

555 Do, H.X., Westra, S., and Leonard, M.: A global-scale investigation of trends in annual maximum  
556 streamflow, *J. Hydrol.*, 552, 28–43, 2017.  
557

558 Donnelly, C., Greuell, W., Andersson, J., Gerten, D., Pisacane, G., Roudier, P., and Ludwig, F.: Impacts  
559 of climate change on European hydrology at 1.5, 2 and 3 degrees mean global warming above  
560 preindustrial level, *Climatic Change*, 19, 1–14, 2017.  
561

562 Drobinski, P., Alonzo, B., Bastin, S., Silva, N. D., and Muller, C.: Scaling of precipitation  
563 extremes with temperature in the French Mediterranean region: what explains the hook shape?,  
564 *J. Geophys. Res.-Atmos.*, 121, 3100–3119, <https://doi.org/10.1002/2015JD023497>, 2016  
565

566 Efron, B.: Bootstrap Methods: Another Look at the Jackknife, *Ann. Stat.*, 7, 1–26, 1979.  
567

568 Giuntoli, I., Renard, B., and Lang, M.: Floods in France. In: Z.W. Kundzewicz, ed. Changes in flood risk  
569 in Europe. Wallingford, UK: IAHS and CRC/Balkema, IAHS Special Publ. 10, 212–224, 2012.  
570

571 Grillakis, M.G., Koutroulis, A.G., Komma, J., Tsanis, I.K., Wagner, W., and Blöschl, G.: Initial  
572 soil moisture effects on flash flood generation - A comparison between basins of contrasting  
573 hydro-climatic conditions, *Journal of Hydrology* 541, 206-217, 2016.  
574

575 Habets, F., Boone, A., Champeaux, J.-L., Etchevers, P., Franchis-teguy, L., Leblois, E., Ledoux, E., Le  
576 Moigne, P., Martin, E., Morel, S., Noilhan, J., Quintana-Segui, P., Rousset-Regimbeau, F., and Viennot,  
577 P.: The SAFRAN-ISBA-MODCOU hydrometeorological model applied over France, *J. Geophys. Res.*,  
578 113, D06113, [doi:10.1029/2007JD008548](https://doi.org/10.1029/2007JD008548), 2008.  
579

580 Hamed, K.H. and Rao, A.R.: A modified Mann-Kendall trend test for autocorrelated data, *J. Hydrol.*, 204,  
581 182–196, 1998.  
582

583 Hodgkins, G. A., Whitfield, P. H., Burn, D. H., Hannaford, J., Renard, B., Stahl, K., Fleig, A. K.,  
584 Madsen, H., Mediero, L., Ko-rhonen, J., Murphy, C., and Wilson, D.: Climate-driven variability in the  
585 occurrence of major floods across North America and Europe, *J. Hydrol.*, 552, 704–717, 2017.  
586

587 Ivancic, T.J., Shaw S.B.: Examining why trends in very heavy precipitation should not be mistaken for  
588 trends in very high river discharge, *Climatic Change*, 133, 681-693, 2015.  
589

590 Jourde, H., Roesch, A., Guinot, V. and Bailly-Comte, V.: Dynamics and contribution of karst  
591 groundwater to surface flow during Mediterranean flood, *Environmental Geology*, 51, 725–730, 2007.  
592

593 Khaliq, M.N., Ouarda, T.B.M.J, Gachon, P., Sushama, L., and St-Hilaire, A.: Identification of  
594 hydrological trends in the presence of serial and cross correlations: A review of selected methods and  
595 their application to annual flow regimes of Canadian rivers, *J. Hydrol.*, 368, 117–130, 2009.

596  
597 Knighton, J.O., DeGaetano, A., and Walter, M.T.: Hydrologic state influence on riverine flood discharge  
598 for a small temperate watershed (Fall Creek, United States): negative feedbacks on the effects of climate  
599 change, *J. Hydrometeorol.*, 18(2), 431–449, 2017.  
600  
601 Koenker, R. and Basset, B.G.: Regression quantiles, *Econometrica*, 46(1), 33–50, 1978.  
602  
603 Koenker, R., Machado J.A.F.: Goodness-of-fit and related inference processes for quantile regression,  
604 *Journal of the American Statistical Association*, 94(448), 1296–1310, 1999.  
605  
606 Kundzewicz, Z.W., Krysanova, V., Dankers, R., Hirabayashi, Y., Kanae, S., Hattermann, F.F., Huang, S.,  
607 Milly, P.C.D., Stoffel, M., Driessen, P.P.J., Matczak, P., Quevauviller, P., and Schellnhuber, H.-J.:  
608 Differences in flood hazard projections in Europe – their causes and consequences for decision making,  
609 *Hydrological Sciences Journal*, 62(1), 1-14, 2017.  
610  
611 Llasat, M.C., Llasat-Botija, M., Petrucci, O., Pasqua, A. A., Rosselló, J., Vinet, F., and Boissier, L.:  
612 Towards a database on societal impact of Mediterranean floods within the framework of the HYMEX  
613 project, *Nat. Hazards Earth Syst. Sci.*, 13, 1337-1350, 2013.  
614  
615 Mann, H. B.: Nonparametric tests against trend, *Econometrica*, 13,245– 259, 1945  
616  
617 Mangini, W., Viglione, A., Hall, J., Hundecha, Y., Ceola, S., Montanari, A., Rogger, M., Salinas, J.L.,  
618 Borzi, I., and Parajka, J.: Detection of trends in magnitude and frequency of flood peaks across Europe,  
619 *Hydrological Sciences Journal*, 63(4), 493-512, 2018.  
620  
621 Mediero, L., Santillán, D., Garrote, L., and Granados, A.: Detection and attribution of trends in magnitude,  
622 frequency and timing of floods in Spain, *J. Hydrol.*, 517, 1072–1088, 2014.  
623  
624 Merz, B., Aerts, J., Arnbjerg-Nielsen, K., Baldi, M., Becker, A., Bichet, A., Blöschl, G., Bouwer, L. M.,  
625 Brauer, A., Cioffi, F., Delgado, J. M., Gocht, M., Guzzetti, F., Harrigan, S., Hirschboeck, K., Kilsby, C.,  
626 Kron, W., Kwon, H.-H., Lall, U., Merz, R., Nissen, K., Salvatti, P., Swierczynski, T., Ulbrich, U.,  
627 Viglione, A., Ward, P. J., Weiler, M., Wilhelm, B., and Nied, M.: Floods and climate: emerging  
628 perspectives for flood risk assessment and management, *Nat. Hazards Earth Syst. Sci.*, 14, 1921-1942,  
629 2014.

630  
631 Meyer, V., Becker, N., Markantonis, V., Schwarze, R., van den Bergh, J. C. J. M., Bouwer, L. M.,  
632 Bubeck, P., Ciavola, P., Genovese, E., Green, C., Hallegatte, S., Kreibich, H., Lequeux, Q., Logar, I.,  
633 Papyrakis, E., Pfuertscheller, C., Poussin, J., Przyluski, V., Thieken, A. H., and Viavattene, C.: Review  
634 article: Assessing the costs of natural hazards – state of the art and knowledge gaps, *Nat. Hazards Earth*  
635 *Syst. Sci.*, 13, 1351-1373, <https://doi.org/10.5194/nhess-13-1351-2013>, 2013.

636  
637 Najibi, N. and Devineni, N.: Recent trends in the frequency and duration of global floods, *Earth Syst.*  
638 *Dynam.*, 9, 757-783, 2018.

639  
640 Neppel L., Bouvier C., Desbordes M., and Vinet F.: A possible origin for the increase in floods in the  
641 Mediterranean region. *Revue des sciences de l'eau* 16(4), 389-494, 2003.

642  
643 Norbiato, D., Borga, M., Esposti, S.D., Gaume, E., and Anquetin, S.: Flash flood warning based on  
644 rainfall thresholds and soil moisture conditions: An assessment for gauged and ungauged basins, *Journal*  
645 *of Hydrology*, 362, 274-290, 2008.

646  
647  
648 Paprotny, D., Sebastian, A., Morales-Nápoles, O., and Jonkman, S. N.: Trends in flood losses in Europe  
649 over the past 150 years, *Nature Communications*, 9(1),1985, doi:10.1038/s41467-018-04253-1, 2018.

650  
651 Paxian, A., Hertig, E., Seubert, S., Vogt, G., Jacobeit, J., and Paeth, H.: Present-day and future  
652 mediterranean precipitation extremes assessed by different statistical approaches, *Clim. Dynam.*, 44,845–  
653 860, <https://doi.org/10.1007/s00382-014-2428-6>, 2015

654  
655 Penna, D., Tromp-van Meerveld, H.J., Gobbi, A., Borga, M., and Dalla Fontana, G.: The influence of soil  
656 moisture on threshold runoff generation processes in an alpine headwater catchment, *Hydrology and Earth*  
657 *System Sciences*, 15, 689-702, 2011.

658  
659 Petrucci, O., Papagiannaki, K., Aceto, L., Boissier, L., Kotroni, V., Grimalt, M., Llasat, M. C.,  
660 Llasat-Botija, M., Rosselló, J., Pasqua, A. A., and Vinet, F.: MEFF: The database of MEditer-ranean  
661 Flood Fatalities (1980 to 2015), *J. Flood Risk Manage.*, e12461, <https://doi.org/10.1111/jfr3.12461>, 2018.

662

663 Pfahl, S., O’Gorman, P. A., and Fischer, E. M.: Under-standing the regional pattern of  
664 projected future changes in extreme precipitation, *Nat. Clim. Change*, 7, 423–  
665 427, <https://doi.org/10.1038/nclimate3287>, 2017.

666

667 Piras, M., Mascaro, G., Deidda, R., and Vivoni, E.R.: Impacts of climate change on precipitation and  
668 discharge extremes through the use of statistical downscaling approaches in a Mediterranean basin,  
669 *Sci. Total Environ.*, 543, 952–964, 2016.

670

671 Polade, S. D., Pierce, D. W., Cayan, D. R., Gershunov, A. and Dettinger, M. D.: The key role of dry days  
672 in changing regional climate and precipitation regimes, *Sci. Rep.* 4, 4364, 2014.

673

674 Polade, S.D., Gershunov, A., Cayan, D.R., Dettinger, M.D., and Pierce, D.W.: Precipitation in a warming  
675 world: Assessing projected hydro-climate changes in California and other Mediterranean climate regions,  
676 *Scientific Reports* 7, 10783, doi:10.1038/s41598-017-11285-y, 2017.

677

678 Quintana-Seguí, P., Habets, F., and Martin, E.: Comparison of past and future Mediterranean high and low  
679 extremes of precipitation and river flow projected using different statistical downscaling methods, *Nat.*  
680 *Hazards Earth Syst. Sci.*, 11, 1411-1432, 2011.

681

682 Quintana-Seguí, P., Le Moigne, P., Durand, Y., Martin, E., Habets, F., Baillon, M., Canellas, C.,  
683 Franchisteguy, L., and Morel, S.: Analysis of Near-Surface Atmospheric Variables : Validation of the  
684 SAFRAN Analysis over France, *J. Appl. Meteor. Climatol.*, 47, 92-107, 2008.

685

686 Raynaud, D., Thielen, J., Salamon, P., Burek, P., Anquetin, S., and Alfieri, L.: A dynamic runoff  
687 coefficient to improve flash flood early warning in Europe: validation on the 2013 Central Euro-pean  
688 floods in Germany. *Met. Apps*, 22: 410-418, 2015.

689

690 Renard, B., Lang, M., Bois, P., Dupeyrat, A., Mestre, O., Niel, H., Sauquet, E., Prudhomme, C., Parey, S.,  
691 Paquet, E., Neppel, L., and Gailhard, J.: Regional methods for trend detection: assessing field significance  
692 and regional consistency, *Water Resour. Res.*, 44, W08419, doi:10.1029/2007WR006268, 2008.

693

694 Ribes, A., Soulihanh, T., Vautard, R., Dubuisson, B., Somot, S., Colin, J., Planton, S., and Soubeyroux, J-  
695 M. : Observed increase in extreme daily rainfall in the French Mediterranean. *Clim Dyn.* 52, 1095-1114,  
696 2019.

697  
698 Rivoire, P., Trambly, Y., Neppel, L., Hertig, E., and Vicente-Serrano, S. M.: Impact of the dry-day  
699 definition on Mediterranean extreme dry-spell analysis, *Nat. Hazards Earth Syst. Sci.*, 19, 1629–1638,  
700 <https://doi.org/10.5194/nhess-19-1629-2019>, 2019.

701 Ruin, I., Creutin, J.-D., Anquetin, S. and Lutoff, C.: Human exposure to flash-floods - Relation between  
702 flood parameters and human vulnerability during a storm of September 2002 in southern France,  
703 *J. Hydrol.*, 361, 199-213, 2008.

704

705 Saint-Martin, C., Javelle, P., and Vinet, F.: DamaGIS: a multisource geodatabase for collection of flood-  
706 related damage data, *Earth Syst. Sci. Data*, 10, 1019-1029, <https://doi.org/10.5194/essd-10-1019-2018>,  
707 2018.

708

709 Sauquet, E. and Catalogne, C.: Comparison of catchment grouping methods for flow duration curve  
710 estimation at ungauged sites in France, *Hydrol. Earth Syst. Sci.*, 15, 2421-2435,  
711 <https://doi.org/10.5194/hess-15-2421-2011>, 2011.

712

713 Sen, P.K.: Estimates of the regression coefficient based on Kendall's tau, *J. Am. Stat. Assoc.*,  
714 63, 1379–1389, 1968

715

716 Schomburgk S., Allier D., and Seguin J.J.: The new aquifer Reference system BDLISA in France and the  
717 representation of karst units : challenges of small-scale mapping, in *Grundwasser - Mensch - Ökosysteme*.  
718 25. Tagung des Fachsektion Hydrogeologie in der DGGV 2016, Karlsruher Institut für Technologie  
719 (KIT), 13. -17. April 2016, Germany. KIT Scientific Publishing. n° ISBN : 978-3-7315-0475-7, 2016.

720

721 Sharma, A., Wasko, C., & Lettenmaier, D.P.: If precipitation extremes are increasing, why aren't floods?  
722 *Water Resources Research*, 54, 8545–8551, 2018.

723

724 Snelder, T. H., Datry, T., Lamouroux, N., Larned, S. T., Sauquet, E., Pella, H., and Catalogne, C.:  
725 Regionalization of patterns of flow intermittence from gauging station records, *Hydrol. Earth Syst. Sci.*,  
726 17, 2685-2699, <https://doi.org/10.5194/hess-17-2685-2013>, 2013.

727

728 Thober, S., Kumar, R., Wanders, N., Marx, A., Pan, M., Rakovec, O., Samaniego, L., Sheffield, J.,  
729 Wood, E. F., and Zink, M.: Multi-model ensemble projections of European river floods and high flows  
730 at 1.5, 2, and 3 degree global warming, *Environ. Res. Lett.*, 13, 1–22, 2018.

731  
732 Tramblay Y., Somot S.: Future evolution of extreme precipitation in the Mediterranean, *Climatic Change*  
733 151(2), 289–302, 2018.  
734  
735 Tramblay, Y., Neppel, L., Carreau, J., and Najib, K.: Non-stationary frequency analysis of heavy rainfall  
736 events in southern France, *Hydrol. Sci. J.*, 58, 1–15, 2013.  
737  
738 Tramblay, Y., Bouvier, C., Martin, C., Didon-Lescot, J.F., Todorovik, D., and Domergue, J. M.:  
739 Assessment of initial soil moisture conditions for event-based rainfall-runoff modelling, *J. Hydrol.*, 387,  
740 176-187, 2010.  
741  
742 Uber, M., Vandervaere, J.-P., Zin, I., Braud, I., Heistermann, M., Legoût, C., Molinié, G., and Nord, G.:  
743 How does initial soil moisture influence the hydrological response? A case study from southern France,  
744 *Hydrol. Earth Syst. Sci.*, 22, 6127-6146, <https://doi.org/10.5194/hess-22-6127-2018>, 2018.  
745  
746 Vicente-Serrano, S.M., Azorin-Molina, C., Sanchez-Lorenzo, A., Revuelto, J., López-Moreno, J.I.,  
747 González-Hidalgo, J.C., and Espejo, F.: Reference evapotranspiration variability and trends in Spain,  
748 1961–2011. *Global and Planetary Change*, 121, 26–40, 2014.  
749  
750 Vidal, J.-P., Martin, E., Kitova, N., Najac, J., and Soubeyroux, J.-M.: Evolution of spatio-temporal  
751 drought characteristics: validation, projections and effect of adaptation scenarios, *Hydrol. Earth Syst. Sci.*,  
752 16, 2935-2955, <https://doi.org/10.5194/hess-16-2935-2012>, 2012.  
753  
754 Viglione, A., Merz, R., and Blöschl, G.: On the role of the runoff coefficient in the mapping of rainfall to  
755 flood return periods, *Hydrol. Earth Syst. Sci.*, 13, 577-593, <https://doi.org/10.5194/hess-13-577-2009>,  
756 2009.  
757  
758 Villarini G. and Slater L.: Examination of Changes in Annual Maximum Gauge Height in the Continental  
759 United States Using Quantile Regression. *J. Hydrol. Eng.*, DOI:10.1061/(ASCE)HE.1943-5584.0001620,  
760 2017.  
761  
762 Vinet, F.: Flood Risk Assessment and Management in France. The Case of Mediterranean Basins, *Flood*  
763 *Prevention and Remediation*. WIT Press, Southampton, UK, p. 105–132, 2011.  
764



765 Vinet F. and Meschinet de Richemond N.: Changes in Flood Risk: Retrospective and Prospective  
766 Approach, Chap. 14 in F. VINET (ed.) Floods 1: risk knowledge ISTE edition London, p. 311-323, 2017.  
767

768 Wasko C, Parinussa R.M., and Sharma A.: A quasi-global assessment of changes in remotely sensed  
769 rainfall extremes with temperature, *Geophys Res Lett* 43:12, 659–612,668, 2016.  
770

771 Wasko, C. and Sharma, A.: Global assessment of flood and storm extremes with increased temperatures,  
772 *Sci Rep*, 7(1), 7945, doi:10.1038/s41598-017-08481-1, 2017.  
773

774 Wasko C. and Nathan R.: Influence of changes in rainfall and soil moisture on trends in flooding, *J.*  
775 *Hydrol.*, 575, 432-441, 2019.  
776

777 Westra, S., Alexander, L. V., and Zwiers, F. W.: Global increasing trends in annual maximum daily  
778 precipitation, *J. Climate*, 26, 3904–3918, 2013  
779

780 Whitfield, P.: Changing floods in future climates. *J. Flood Risk Manage*, 5: 336-365, 2012.  
781

782 Wilks, D.S.: The stippling shows statistically significant grid points: how research results are routinely  
783 overstated and over interpreted, and what to do about it, *Bull. Am. Meteorol. Soc.*, 97, 2263–2273, 2016.  
784

785 Woldemeskel, F. and Sharma, A.: Should flood regimes change in a warming climate? The role of  
786 antecedent moisture conditions, *Geophys. Res. Lett.*, 43, 7556–7563, doi:10.1002/2016GL069448, 2016.  
787

788 Yin, J., Gentine, P., Zhou, S., Sullivan, S.C., Wang, R., Zhang, Y., and Guo, S.: Large increase in global  
789 storm runoff extremes driven by climate and anthropogenic changes. *Nat. Commun.* 9, 4389,  
790 DOI:10.1038/s41467-018-06765-2, 2018.  
791

792 Zhang, Y., Wei, H., and Nearing, M. A.: Effects of antecedent soil moisture on runoff modeling in small  
793 semiarid watersheds of southeastern Arizona, *Hydrol. Earth Syst. Sci.*, 15, 3171-3179,  
794 <https://doi.org/10.5194/hess-15-3171-2011>, 2011.  
795  
796  
797  
798

799  
800  
801  
802  
803

**Table 1:** summary of the trend detection on different variables: number of positive, negative trends significant at the 10% level and regional significance

	Variable	Positive trends	Negative trends	Regional significance
Climatic variables	Mean precipitation	0	56	Yes (28 basins)
	Mean rainfall	1	49	Yes (20 basins)
	Frequency of dry days	46	2	Yes (9 basins)
	Mean temperature	166	0	Yes (165 basins)
	Mean surface soil moisture	1	132	Yes (129 basins)
	Mean root zone soil moisture	1	132	Yes (129 basins)
	Mean actual evapotranspiration	169	0	Yes (169 basins)
	Mean reference evapotranspiration	136	0	Yes (131 basins)
Flood events	Number of floods above the 95th percentile	0	67	Yes (40 basins)
	Number of floods above the 99th percentile	1	45	Yes (7 basins)
	Flood magnitudes above the 95th percentile	4	3	No
	Flood magnitudes above the 99th percentile	16	5	No
Climatic variables associated with flood events	Cumulative precipitation during floods above the 95th percentile	36	6	Yes (16 basins)
	Cumulative precipitation during floods above the 99th percentile	34	3	Yes (5 basins)
	Antecedent wetness conditions for floods above the 95th percentile	10	40	Yes (11 basins)
	Antecedent wetness conditions for floods above the 95th percentile	6	24	Yes (14 basins)

804  
805  
806  
807  
808  
809

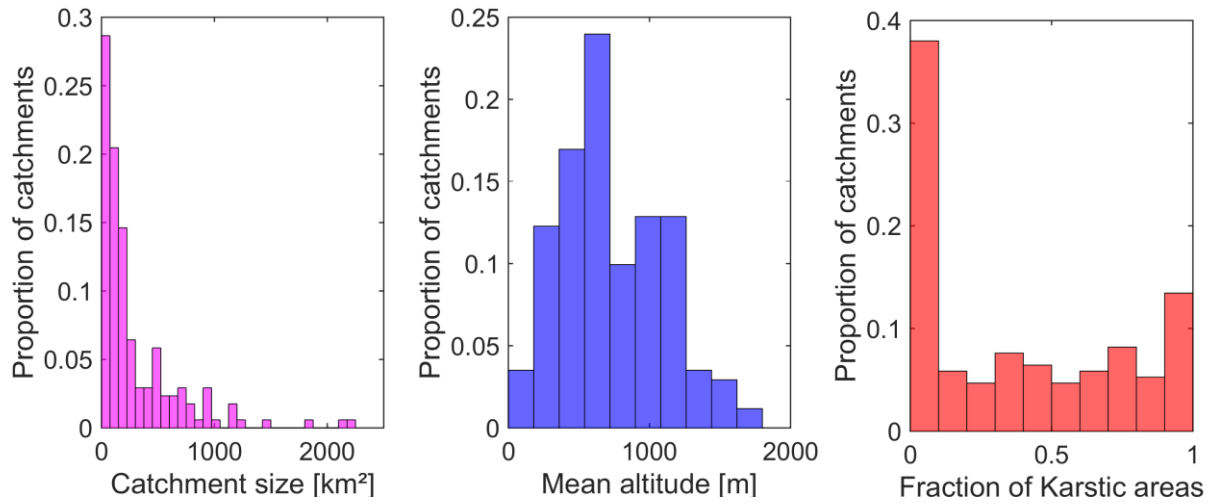
810

811

812 **FIGURES**

813

814



815

816

817 Figure 1: Catchment size, mean altitude and fraction of karstic areas

818

819

820

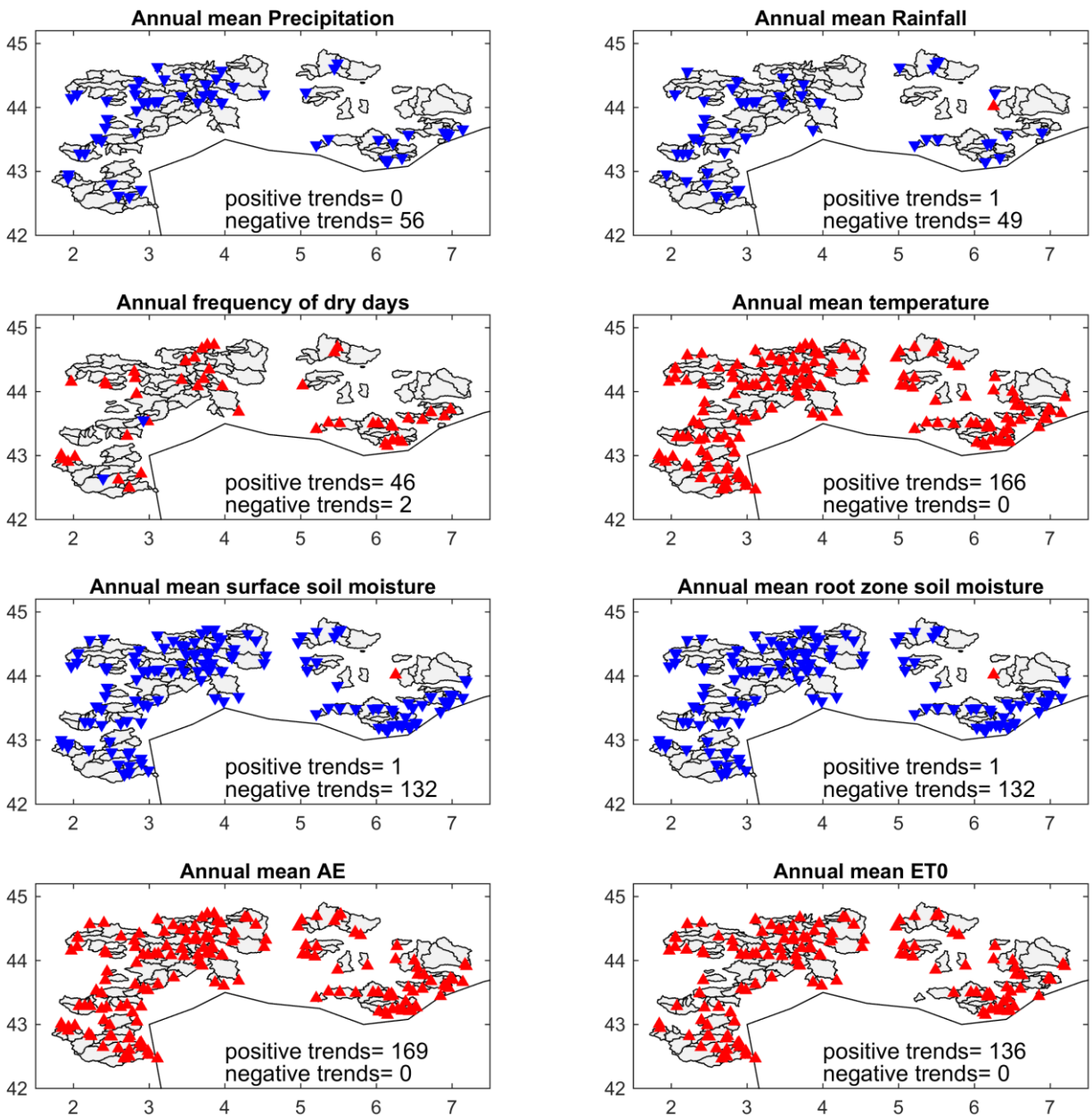
821

822

823

824

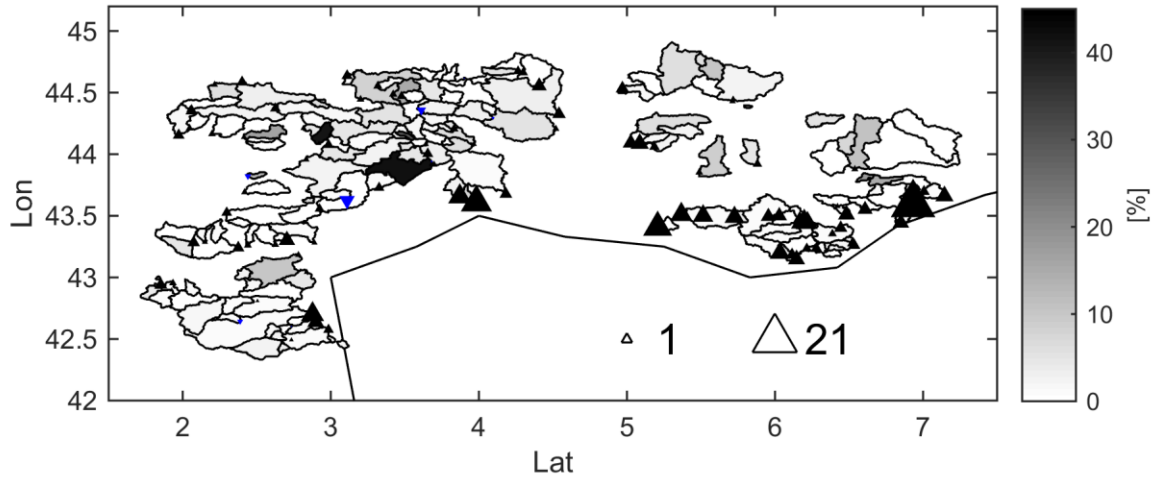
825



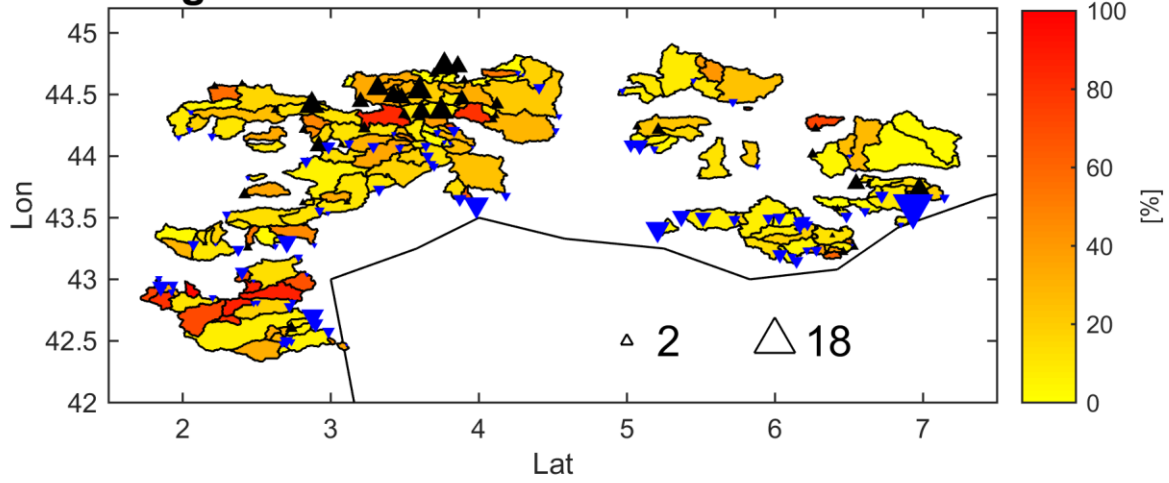
826  
 827 Figure 2: Significant annual trends at the 10% level (Mann Kendall test) between 1958 and 2018  
 828 in precipitation, rainfall, frequency of dry days (with precipitation below 1mm), temperature, soil  
 829 moisture, actual evapotranspiration (AE) and reference evapotranspiration (ET0)

830  
 831  
 832  
 833

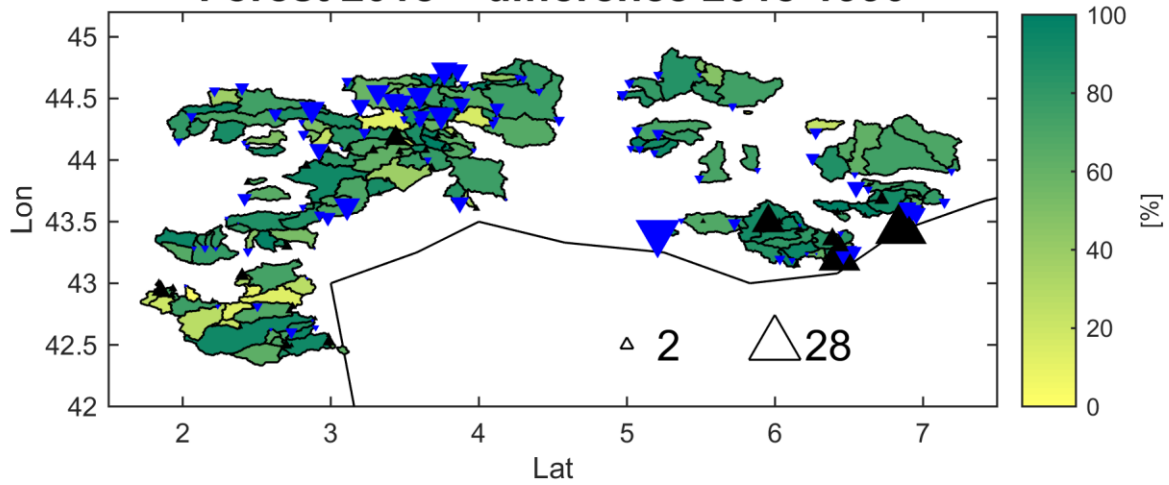
### Urban 2018 + difference 2018-1990



### Agriculture 2018 + difference 2018-1990



### Forest 2018 + difference 2018-1990



834

835

836

837

838 Figure 3: Urban, Agricultural and Forest cover by catchment from the CORINE database for the  
839 year 2018 and difference between 1990 and 2018 (upward black triangles indicate an increase,  
840 downward blue triangles a decrease, the triangle size are proportional to the absolute changes  
841 between 1990 and 2018).

842

843

844

845

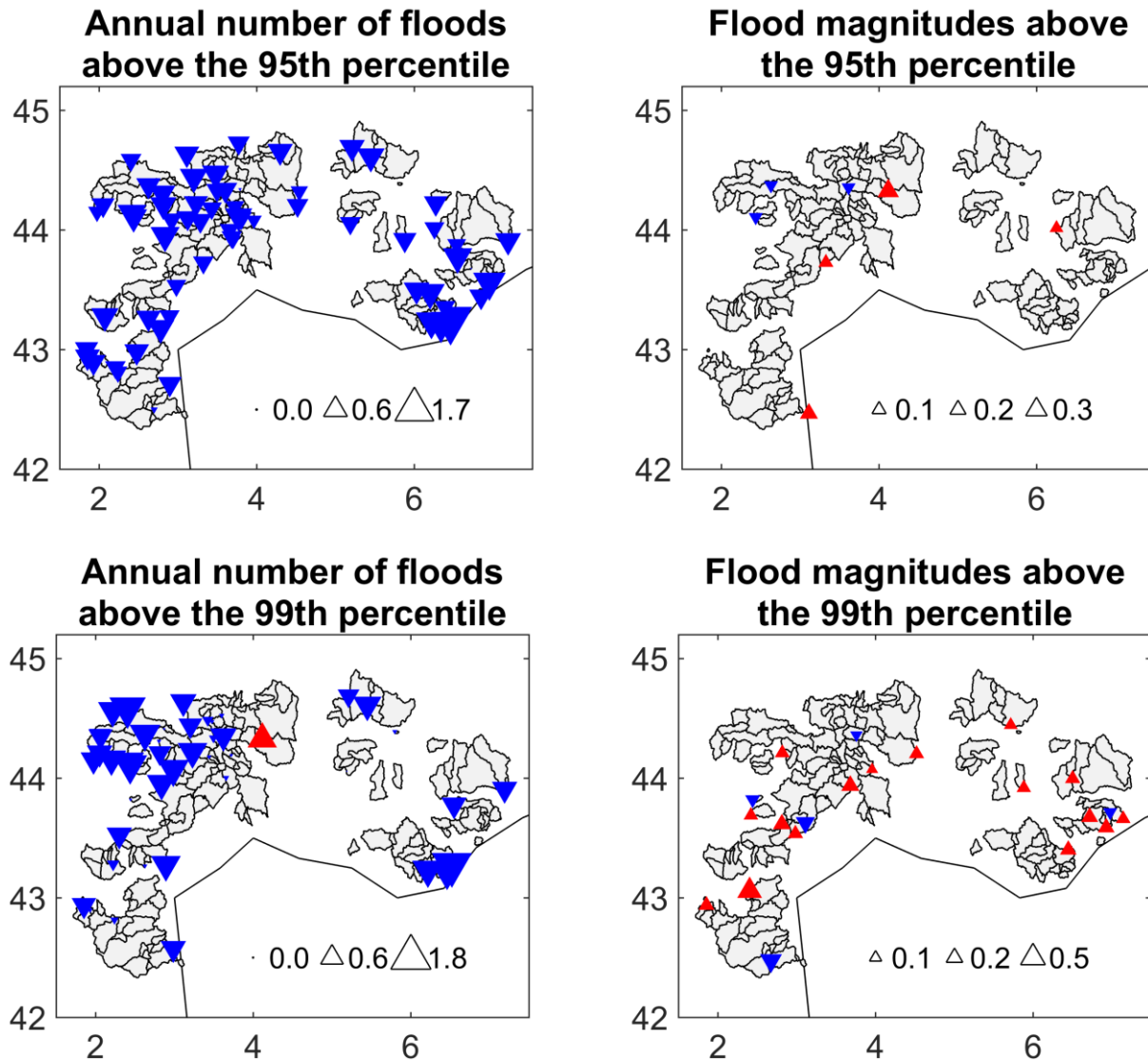
846

847

848

849

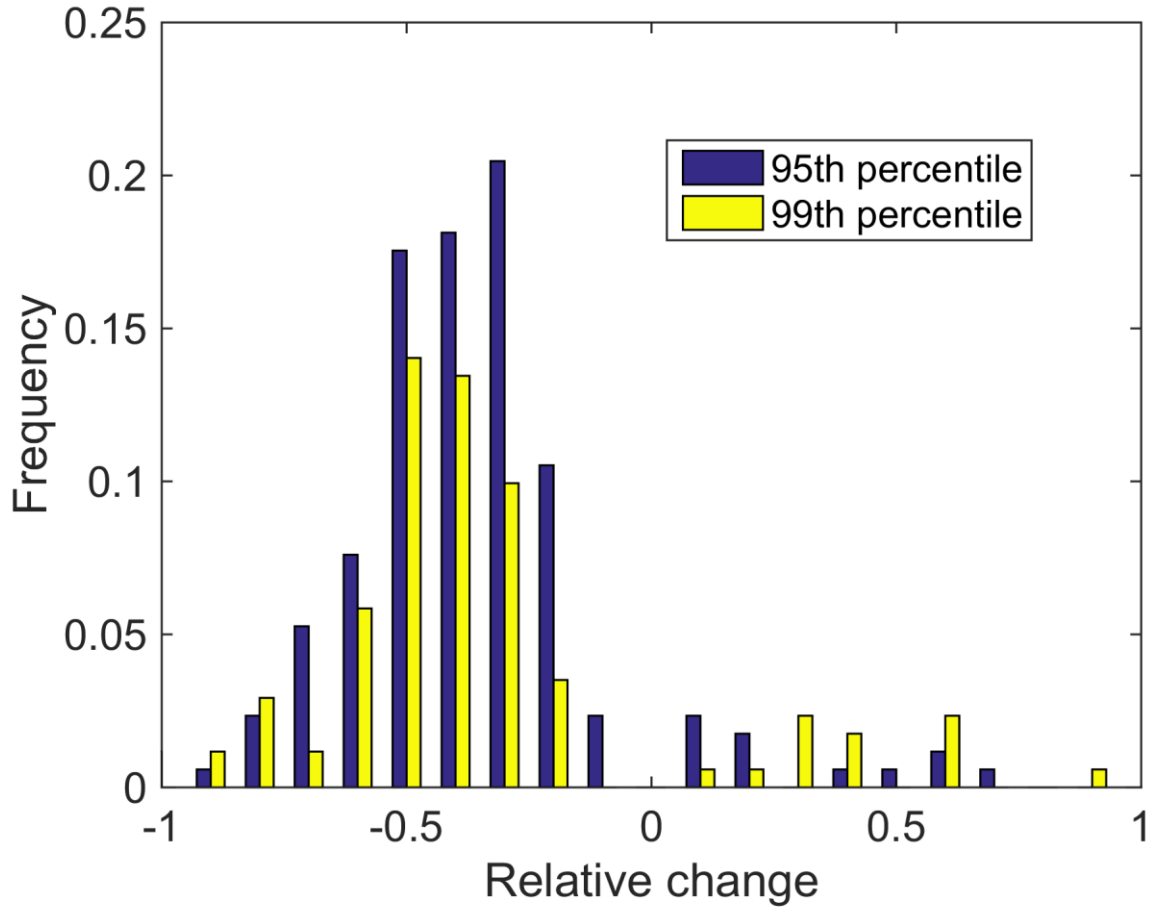
850



851  
 852  
 853  
 854 Figure 4: Significant trends at the 10% level (Mann Kendall test) in the annual number of flood  
 855 events above the 95<sup>th</sup> and 99<sup>th</sup> percentiles (left) and in the magnitude of these threshold  
 856 exceedances (right). Blue triangles indicate a decrease and red triangles an increase. The size of  
 857 the triangles indicates the relative changes.

858  
 859  
 860  
 861

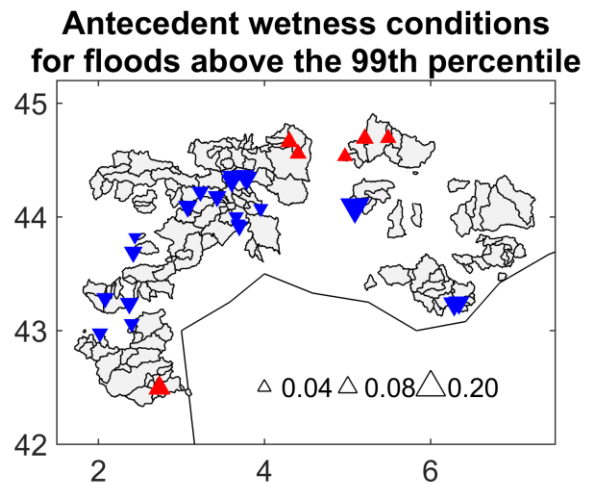
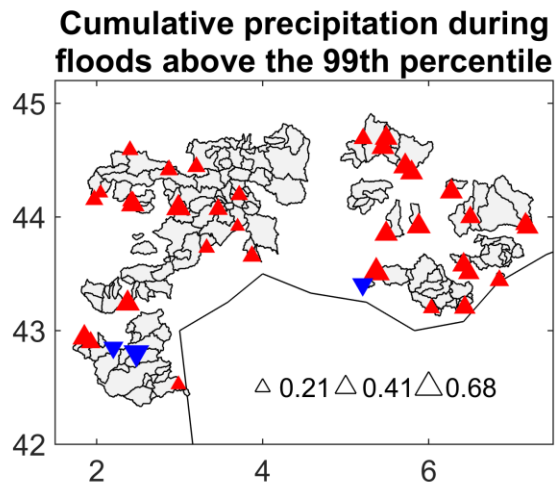
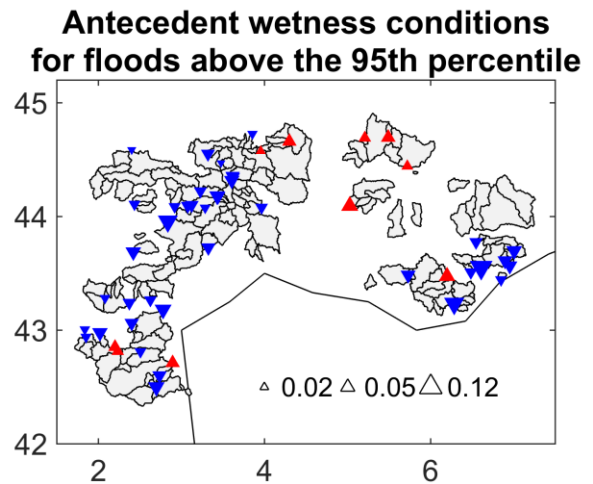
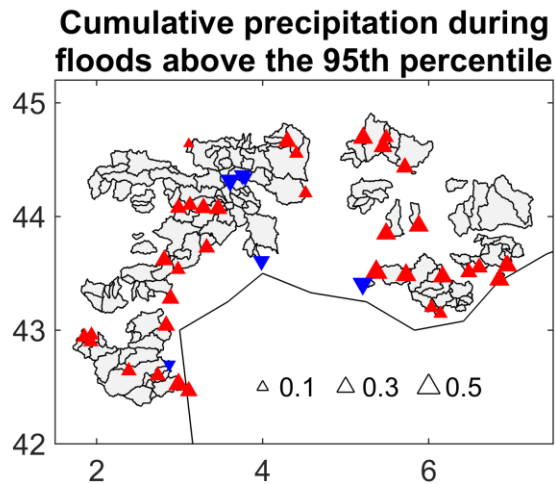
862  
863  
864



865  
866  
867  
868  
869  
870  
871  
872  
873  
874  
875  
876

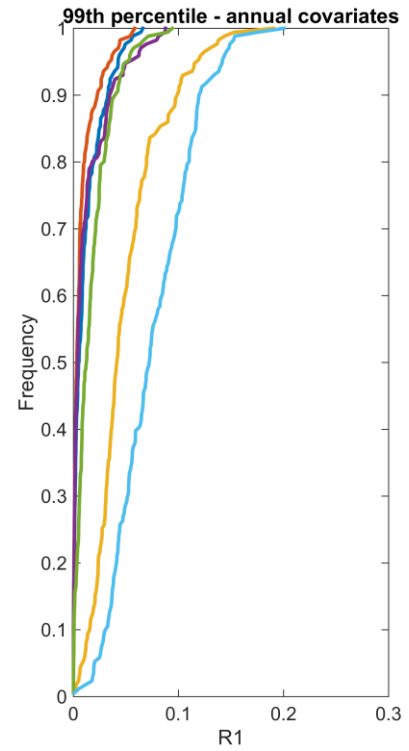
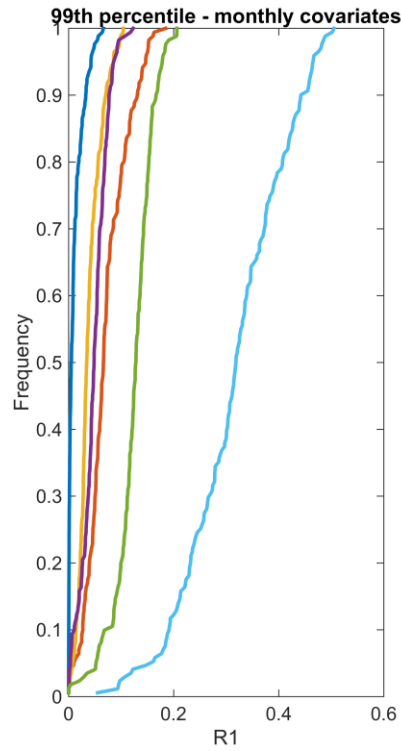
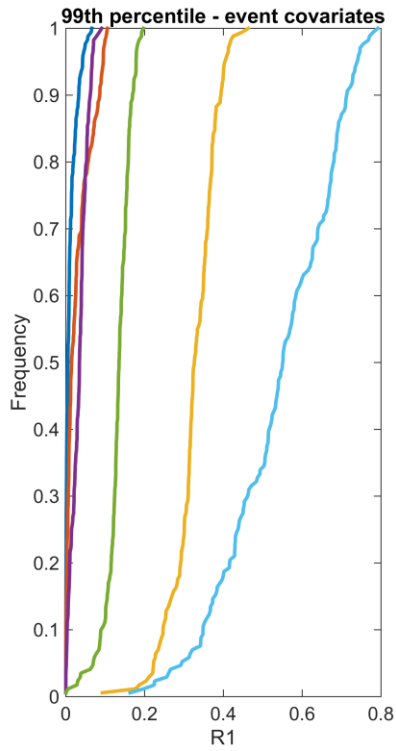
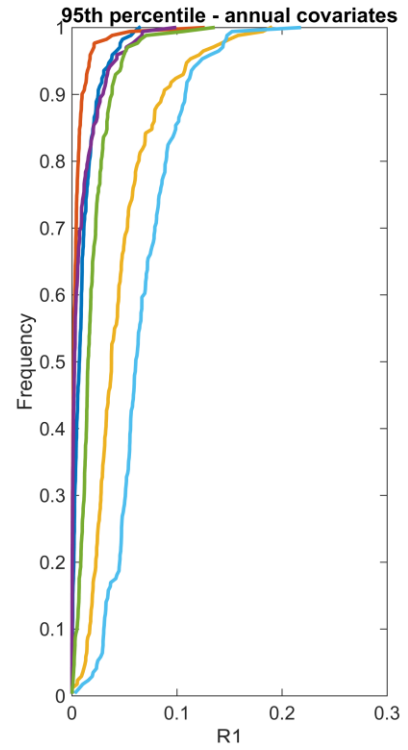
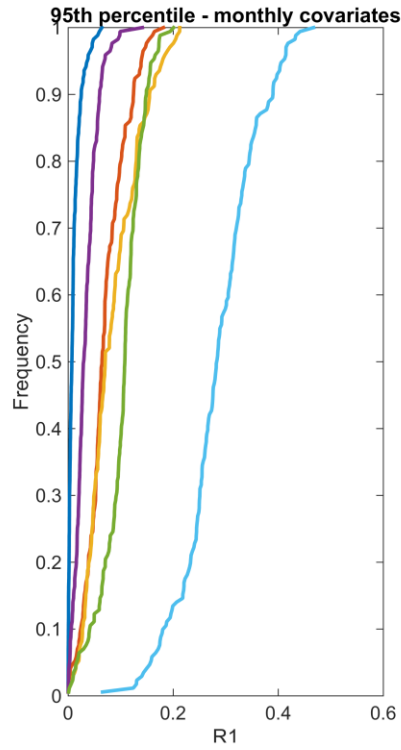
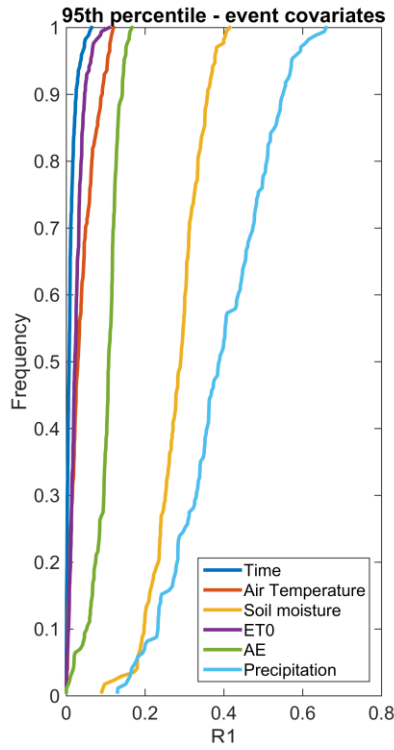
Figure 5: Histogram of the relative changes in the 95<sup>th</sup> and 99<sup>th</sup> percentiles estimated from the quantile regression models with time as covariate (with a slope significantly different than zero at the 10% level)





877  
878  
879  
880  
881  
882  
883  
884  
885  
886  
887  
888  
889

Figure 6: Significant trends at the 10% level (Mann Kendall test) in cumulative precipitation during flood events above the 95<sup>th</sup> and 99<sup>th</sup> percentile (left) and in the soil moisture initial conditions (right). Blue triangles indicate a decrease and red triangles an increase. The size of the triangles indicates the relative changes.



891 Figure 7: Distribution of the  $R^I$  coefficients for different covariates for the 95<sup>th</sup> or 99<sup>th</sup> percentiles  
892 of daily runoff, averaged at: (i) the event scale (3 days), left panels, (ii) the monthly scale, central  
893 panels, and (ii) annual timescale, right panels.  
894